ADVANCED FUNCTIONAL MATERIALS
www.afm-journal.de

Conjugated Polyelectrolyte and Aptamer Based Potassium Assay via Single- and Two-Step Fluorescence Energy Transfer with a Tunable Dynamic Detection Range

*Bao Lam Nguyen, Ji-Eun Jeong, In Hwan Jung, Boram Kim, Van Sang Le, Inhong Kim, Kwangseuk Kyhm, and Han Young Woo**

A new potassium ion detection assay was developed using a dye-labeled aptamer and conjugated polyelectrolyte (CPE) as a signaling platform via 1-step and 2-step fluorescence resonance energy transfer. Guanine-rich K^+-specific aptamers were designed as K^+ ion recognition species with 6-carboxyfluorescein (6-FAM) and 6-carboxytetramethylrhodamine (6-TAMRA) at both termini. In the presence of K^+ ions, the aptamers undergo a conformational change from an unfolded to folded form by forming a G-quadruplex with K^+, bringing two dyes in proximity. FRET-induced 6-TAMRA emission was proportional to [K^+] in a range of 22.5 μM–100 mM in water without interference by the presence of excess Na^+ ions (100 mM). Upon the addition of CPE, a two-step FRET process from CPE to 6-TAMRA via 6-FAM was enabled, showing an intensified 6-TAMRA signal with K^+ ions. The dynamic detection range and limit of detection (LOD) was fine-tuned from ~millimolar to ~nanomolar concentrations of K^+ by modulating the signal amplification effect of CPE. The LOD was determined to be ≈3.0 nM. This detection assay also showed high selectivity against other metal ions. This sensing scheme can be extended to the detection of a wide range of target materials by simply modifying the recognition aptamer sequence.

1. Introduction

Conjugated polyelectrolytes (CPEs) have found many applications in chemical and biological sensors due to their unique electrical and optical properties.[1] Furthermore, CPEs are used as an optical antenna for signal amplification because of their intrinsic light harvesting or molecular wire effect.[2] A wide range of CPEs have been designed and studied by a combination with targeting moieties to detect chemicals and biological molecules, such as DNA, RNA, peptide, ATP, thrombin, and so forth, by taking advantage of their signal amplification properties.[3]

Aptamers are oligonucleotides that bind selectively to a specific target molecule with high affinity and specificity.[4] Some specific single-stranded aptamers with guanine (G)-rich base sequences can transform from an unfolded to secondary folded structure, G-quadruplex, in the presence of specific alkali metal ions via intramolecular hydrogen bonding.[5] In particular, potassium ions promote this transformation.[6] Extensive studies have focused on developing aptamer-based probe systems for detecting metal ions and/or biomolecular species.[7] On the other hand, the narrow dynamic range (i.e., interval of the analyte that gives the input/output response curve) is one notable limitation when using the conformational changes in aptamers for chemo- or biosensors.[8] Many studies have focused on tuning or broadening the useful dynamic range.[9] To develop efficient sensors, high selectivity, sensitivity and a broad/controllable dynamic detection range should be considered together.

The fluorescence resonance energy transfer (FRET) mechanism is used widely for the design of various sensory schemes.[10] In addition to conventional single-step FRET (one donor and one acceptor), two-step and multi-step FRET-based sensory systems have been developed because of ability to probe more complicated systems, high efficiency with long range energy transfer, large Stokes shift, and high sensitivity.[11] On the other hand, the design and application of two (or multi)-step FRET based detection systems with high selectivity and sensitivity, is still a challenge.

B. L. Nguyen, J.-E. Jeong, B. Kim, V. S. Le, Prof. H. Y. Woo
Department of Nanofusion Engineering and Department of Cogno-Mechatronics Engineering (WCU)
Pusan National University
Miryang, 627–706, Republic of Korea
E-mail: hywoo@pusan.ac.kr
B. L. Nguyen
Institute of Applied Materials Science
Vietnam Academy of Science and Technology
Ho Chi Minh City, Vietnam
I. H. Jung
Department of Chemistry
University of Chicago
Chicago, IL, 60637, USA
I. Kim, Prof. K. Kyhm
Department of Cogno-Mechatronics Engineering
Physics Education and Physics
Pusan National University
Busan, 609–735, Republic of Korea

DOI: 10.1002/adfm.201301515

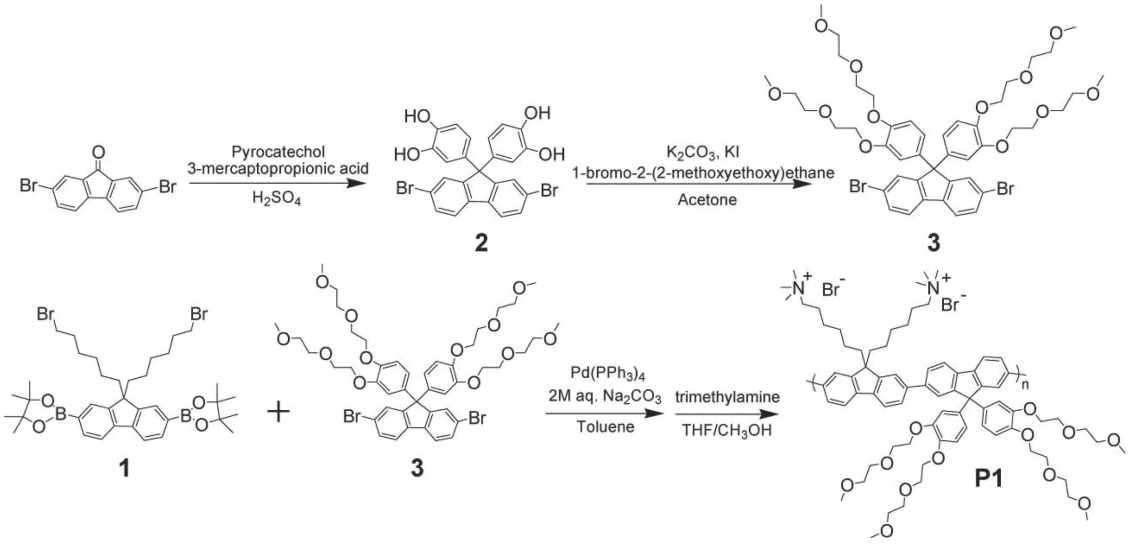

Scheme 1. Synthetic route to cationic CPE (**P1**).

The potassium ion is a physiologically important and predominant intracellular cation. Apoptosis is related to the decrease in extracellular K^+ ions,[12] whereas an increase in K^+ ions can lead to hyperexcitability. Potassium also plays an important role in other biological processes, such as nerve transmission, maintaining muscular strength and enzyme activation, and so forth.[13] Considerable effort has been made to develop bioassays to detect K^+ ions.[14] Nevertheless, there are still problems that need to be solved, including effective detection in aqueous media, high selectivity against other intra- and extracellular cations (e.g., Na^+), high detection sensitivity and tunable detection range.

Herein, we report a new K^+ ion detection assay combining a K^+-specific biomolecule (aptamer) as a recognizing probe and a synthetic polymer with tunable optical properties. A highly sensitive and selective one- and two-step FRET based sensory scheme was designed with a tunable sensing range and limit of detection (LOD). Three types of K^+-specific aptamers were designed as a K^+-specific probe with 6-carboxyfluorescein (6-FAM) and 6-carboxytetramethylrhodamine (6-TAMRA) at both termini. Cationic polyfluorene-based CPE, as an optical antenna, was designed carefully with side chains containing ionic groups and ethylene oxide units for solubility in water.[15] The presence of K^+ ions induced a structural transformation of a linear aptamer into a folded G-quadruplex form, bringing two dyes at both termini into close proximity, thereby enabling efficient FRET from 6-FAM to 6-TAMRA. The FRET-induced 6-TAMRA emission intensified linearly with increasing $[K^+]$ in the range of millimolar concentrations. Interestingly, the sensor characteristics (such as the dynamic detection range and detection limit) could be fine-tuned via a two-step FRET process by the addition of CPEs as a signal amplifier. The detection range was extended successfully to micromolar and nanomolar concentrations of K^+ ions by modulating the antenna effect of CPEs. More importantly, this sensor scheme can be applied to the detection of other target molecules simply by modifying the aptamer unit in the probe.

2. Result and Discussion

The solubility of CPEs in water and their interactions with biomolecules are decisive for biological applications. The optical characteristics of the CPE are also dependent strongly on their solubility in aqueous media.[16] On the other hand, hydrophobic interactions also play an important role in the interactions between CPEs and biomolecules. Therefore, a new cationic fluorene-based CPE (**P1**) was designed and synthesized carefully as an optical platform for chemo- and biosensor applications. To improve the water solubility, both ionic tetraalkylammonium bromide and ethylene oxide units were incorporated in the side chains. In addition, the phenylene rings were also incorporated into the polymeric backbone to enhance the hydrophobic interactions with oligonucleotides.[17] **Scheme 1** shows the synthetic route to the monomers and polymer, **P1**. The polyfluorene-based cationic **P1** was synthesized via a Suzuki coupling reaction of 2,7-bis(4,4,5,5-tetramethyl-1,3,2-dioxaborolan-2-yl)-9,9-bis(6′-bromohexyl)fluorene (1) and 2,7-dibromo-9,9-bis(3,4-bis(2-(2-methoxyethoxy)ethoxy)phenyl)fluorene (3) using $(PPh_3)_4Pd(0)$ as a catalyst in toluene/water (2:1, volume ratio) at 85 °C for 36 h (yield: 66%), followed by successive quaternization with condensed trimethylamine at room temperature (yield: 85%). The number–average (M_n) and weight-average molecular weights (M_w) were determined to be 25 000 g mol^{-1} and 31 000 g mol^{-1} (PDI = 1.26), with the neutral precursor of **P1**.

Figure 1 shows the UV-vis absorption and photoluminescence (PL) spectra of **P1** in water. The maxima of the UV and PL spectra of **P1** were observed at λ_{abs} = 391 nm and λ_{PL} = 425 nm. The measured molar absorption coefficient and PL quantum efficiency of **P1** was 5.2×10^4 M^{-1} cm^{-1} and ≈0.58, respectively. The PL quantum efficiency of **P1** in water is higher than those (0.4–0.5) of similar structures reported previously.[18] Good spectral overlap was noted between the emission and absorption of **P1** (FRET donor) and 6-FAM (intermediate FRET acceptor), and between 6-FAM (intermediate FRET donor) and 6-TAMRA (FRET acceptor). To determine the solubility of **P1** in water,

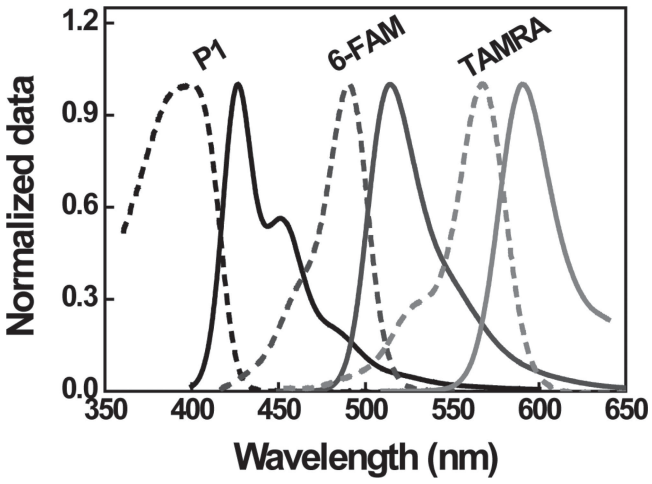

Figure 1. Normalized absorption (dash) and emission (solid) spectra of **P1**, 6-FAM, and 6-TAMRA in water.

a stock solution of **P1** in dimethylsulfoxide (DMSO) was prepared (5×10^{-4} M), which was diluted to 2.5×10^{-7}–2.5×10^{-5} M in water. The PL spectra of the resulting solution were measured at 425 nm (which is the max. PL wavelength of **P1**) with chainging [**P1**] (Figure S1, Supporting Information). In all experiments, the DMSO content was maintained at 0.12 vol% in water, to eliminate the organic solvent effects on solubility.[19] The solubility of **P1** was estimated to be 5 μM in water by measuring the PL intensity with increasing [**P1**].

Scheme 2 illustrates the detection strategy for K^+ ions in water. The guanine (G)-rich K^+-specific aptamer containing 15 bases (GGTT GGTG TGGT TGG) was used as a K^+ recognizing unit that forms a G-quadruplex in the presence of K^+ ions.[20] Three types of K^+-specific probes were designed, where

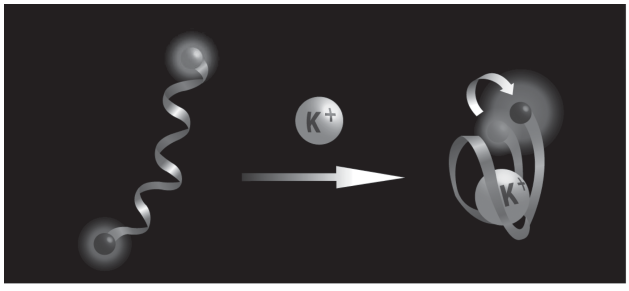

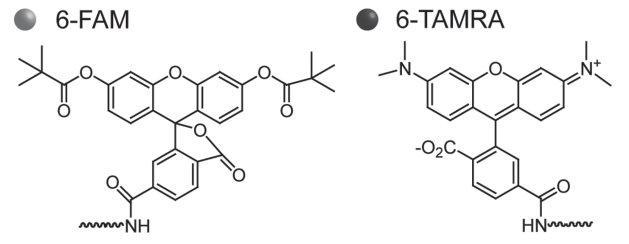

Aptamer 1 : 5' [6-FAM] GGTT GGTG TGGT TGG [6-TAMRA] 3'
Aptamer 2 : 5' [6-FAM] TTTT AGGT TGGT GTGG TTGG [6-TAMRA] 3'
Aptamer 3 : 5' [6-FAM] TTTT ATTT TAGG TTGG TGTG GTTG GTTT TA [6-TAMRA] 3'

Scheme 2. Potassium ion detection scheme and molecular structures of three aptamer probes.

the 5′- and 3′-termini of the aptamer were labeled with 6-FAM and 6-TAMRA, respectively. To compare the FRET-based sensor properties, single and dual spacer groups were introduced to aptamers 2 and 3 to tune the intermolecular separation between the two dyes. In the absence of K^+ ions, the aptamers remain mainly in a linear form, where FRET from 6-FAM to 6-TAMRA occurs inefficiently and weak FRET-induced 6-TAMRA emission is expected. In the presence of K^+ ions, the aptamers undergo a conformational change from an unfolded linear form to the folded G-quadruplex structure, bringing the two dyes in proximity. Once 6-FAM is excited, efficient FRET from 6-FAM to 6-TAMRA occurs with strong FRET-induced 6-TAMRA emission. The conformational change in the aptamer with/without K^+ ions induces a change in the FRET signal, enabling sensitive and selective potassium detection.

Figure 2 shows the FRET-induced PL spectra of the three aptamers in the presence and absence of K^+ ions (50 mM). The PL spectra were measured with a 10 nM aptamer solution in 20 mM Tris-HCl buffer containing 100 mM NaCl as the salt (pH = 7.4). Before the PL measurements, the solution was annealed at 60 °C for 30 min (to ensure the G-quaduplex formation with potassium) and cooled down to room temperature for 1 h. Finally, the PL spectra were measured by exciting 6-FAM at 490 nm. Without K^+ ions, the aptamers exist in a linear form. Among the three aptamers, the FRET-induced emission of 6-TAMRA in aptamer 1 showed the highest intensity compared to those of aptamers 2 and 3. This can be explained by the intermolecular separation between the FRET donor (6-FAM) and acceptor (6-TAMRA). Aptamer 1 has 15 bases between the two dyes, and aptamer 2 and 3 have 20 and 30 bases, respectively. The FRET rate (k_{FRET}) is very sensitive to the intermolecular distance and is inversely proportional to r_{DA}^6 according to:

$$k_{FRET}(r) \propto \frac{Q_D \kappa^2}{\tau_D r_{DA}^6 n^4} \int_0^\infty F_D(\lambda)\varepsilon_A(\lambda)\lambda^4 d\lambda \quad (1)$$

where Q_D is the PL quantum yield of a donor in the absence of a FRET acceptor, κ^2 is related to the relative orientation of the transition dipole moments of a donor and acceptor, the integral part corresponds to spectral overlap between the emission of a donor, $F_D(\lambda)$ and the molar absorptivity of an acceptor, $\varepsilon_A(\lambda)$, τ_D is the PL lifetime of a donor in the absence of an acceptor, r_{DA} is the intermolecular distance between the donor and acceptor (D–A distance), and n is the refractive index of the solvent.

Upon the addition of K^+ ions, the FRET signal was enhanced for all aptamers, and clear turn-on and -off states were observed in the presence and absence of K^+ ions by exciting 6-FAM at 490 nm. Aptamer 1 showed the highest on/off ratio among the three aptamers due to the more efficient FRET in the G-quadruplex structure. On the other hand, aptamers 2 and 3 have one spacer group (TTTT A) and dual spacers (TTTT ATTT TA and TTTT A) at both termini; the two dyes are still expected to be separated in the G-quadruplex with K^+ with the longer intermolecular distance compared to aptamer 1. The higher FRET ratio ($I_{585\ nm}/I_{517\ nm}$) was measured to be 1.72 for aptamer 1 relative to those (0.77, 0.35) of aptamers 2 and 3. **Figure 3** shows the normalized FRET spectra of aptamer 1 with increasing [K^+] = 0–50 mM. With increasing [K^+], the FRET-induced 6-TAMRA emission increased gradually, suggesting the increased formation of the G-quadruplex with potassium

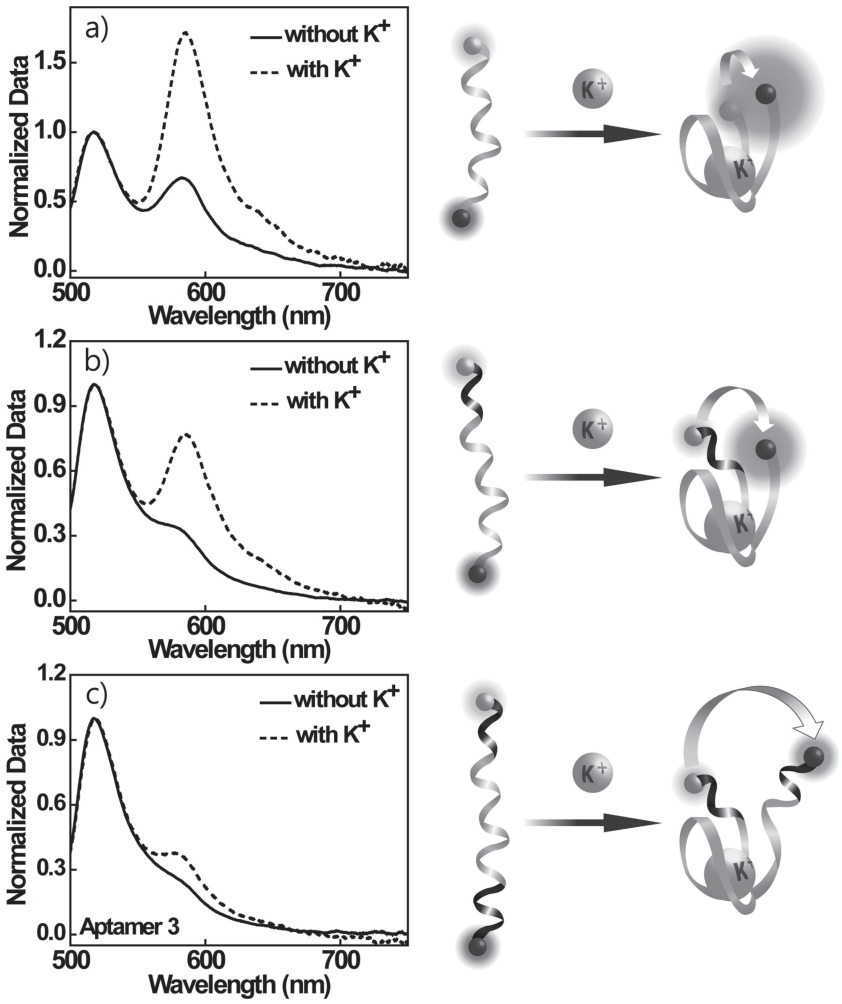

Figure 2. Normalized PL spectra of a) aptamer 1, b) aptamer 2, and c) aptamer 3 in the presence and absence of K^+ ions. [Aptamer] = 10 nM, [K^+] = 50 mM in Tris-HCl buffer (20 mM, pH = 7.4), Excited at 490 nm.

ions. From the calibration curves (Figure 3b and Figure S2, Supporting Information), the LOD was determined to be 22.5 μM, 0.82 mM, and 3.3 mM for aptamer 1, 2, and 3, respectively (3σ/slope, where σ is the standard deviation in 5 independent measurements). The upper limit of the dynamic detection range was determined to be ≈100 mM for the aptamer 1 and 2 systems (**Figure 4**).

The Förster distance (R_0) is defined as the intermolecular distance between the donor and acceptor at which the probability of FRET is 50%. R_0 can be calculated from the spectral overlap of the donor emission and acceptor absorption via

$$R_0^6 = \frac{9000(\ln 10)\kappa^2 Q_D}{128\pi^5 N n^4} \int_0^\infty F_D(\lambda)\varepsilon_A(\lambda)\lambda^4 d\lambda \quad (2)$$

For the fully dynamic system with randomized dipoles by rotational diffusion, κ^2 is assumed to be 2/3. The PL quantum efficiency of **P1** and 6-FAM was determined to be 0.58 and 0.87, respectively in Tris-HCl buffer. The Förster distance was estimated to be R_0 = 44.8 Å for the 6-FAM and 6-TAMRA couples. The intermolecular distance between 6-FAM and 6-TAMRA in free aptamers (without K^+) was calculated to be R = 47 Å, 64 Å, and 98 Å in aptamer 1, 2, and 3, respectively, by considering the intermolecular separation of 3.4 Å between bases. Given the R_0 and R between the D–A pair, the FRET efficiency (E) for free aptamers was estimated to be 0.41, 0.11, and 0.01 in aptamer 1, 2, and 3, respectively, according to

$$E(R) = \frac{1}{1 + (R/R_0)^6} \quad (3)$$

Suppose the PL intensity of free donor is I_D, the PL intensity I_{DA} of donor in the D–A complex separated by R is given as

$$I_{DA}(R) = I_D - E(R)\ I_D \quad (4)$$

Therefore, the PL intensity ratio ($I_{DA}(R')/I_{DA}(R)$) which is measured at the donor side (6-FAM) in the aptamers in the absence (R) and presence (R') of K^+, respectively, can be associated with the distance dependence of FRET efficiency as

$$\frac{I_{DA}(R')}{I_{DA}(R)} = \frac{I_D - E(R')\ I_D}{I_D - E(R)\ I_D} = \frac{1 - E(R')}{1 - E(R)} \quad (5)$$

The FRET efficiency (E) in the presence of K^+ ions was calculated at [K^+] = 150 mM where the FRET signal was saturated and there must be negligible free aptamers. Based on these calculations, one can roughly estimate the FRET efficiency and intermolecular 6-FAM/6-TAMRA distance when the aptamers form the G-quadruplex with K^+ ions. The FRET efficiency and the corresponding intermolecular separation were calculated to be 0.96 (25 Å), 0.87 (32 Å), and 0.73 (38 Å) for aptamer 1, 2, and 3 with K^+ ions (Figure S3, Supporting Information).

Scheme 3 describes the detection strategy for K^+ ions with the aptamer and CPE as the signaling platform. In the presence of K^+ ions, the G-rich aptamer sequence offers the specific recognition for potassium, inducing a structural change from an unfolded form to a folded G-quadruplex. Upon addition of cationic CPE, an electrostatic complex of CPE/G-quadruplex is formed (with close proximity between 6-FAM and 6-TAMRA), where efficient two-step FRET can occur from the CPE to 6-TAMRA via 6-FAM by exciting the CPE, resulting in strong 6-TAMRA emission. Without K^+ ions, the aptamers remain mostly in the linear form after forming an electrostatic complex with CPEs. In this case, two-step FRET is relatively inefficient due to the distance between the two dyes, resulting in weak 6-TAMRA emission by exciting the CPE. Through this simple scheme, the two-step FRET-induced 6-TAMRA emission produces a clear signal turn on and off in the presence or absence of K^+ ions.

The sensor characteristics such as the dynamic detection range and LOD, was modulated successfully by the addition of

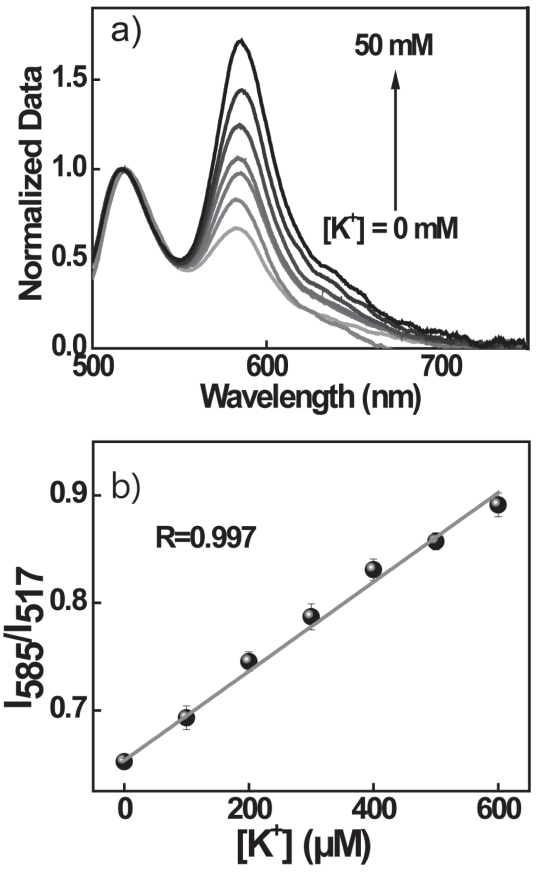

Figure 3. a) Normalized PL spectra of aptamer 1 with increasing [K+]. b) FRET ratio ($I_{585\ nm}/I_{517\ nm}$) vs [K+]. [Aptamer] = 10 nM in Tris-HCl buffer (20 mM, pH = 7.4), Excited at 490 nm.

P1 as an optical antenna on account of its light harvesting effect. **Figure 5** shows the normalized FRET-induced PL spectra of aptamer 1 upon the addition of **P1** in the presence and absence of K^+ ions. Excess **P1** was added to the aptamer solution after annealing with and without K^+ ions. The final **P1** concentration was adjusted to [**P1**] ≈ 4.5×10^{-7} M (based on the repeating unit, charge ratio = [+] in **P1**: [-] in aptamer = 6:1), where all aptamers must be complexed with **P1** through electrostatic and hydrophobic interactions. The two-step FRET-induced PL spectra were measured by exciting **P1** at 390 nm. By exciting **P1**, fluorescence energy transfer from **P1** to 6-FAM and from 6-FAM to 6-TAMRA is enabled, resulting in two-step FRET-induced emission of 6-TAMRA. In the absence of K^+ ions, direct energy transfer from **P1** to 6-TAMRA is also possible due to the spectral overlap between **P1** and 6-TAMRA (Figure S4, Supporting Information). The weak 6-TAMRA PL without K^+ (in Figure 5) must be originated from the direct FRET from **P1** to 6-TAMRA. However, by comparing the FRET-induced 6-TAMRA signals with/without K^+, we can conclude that the 6-TAMRA signal was mainly intensified by the two-step FRET process from **P1** to 6-TAMRA via 6-FAM. The Förster distance was also estimated to be 33.1 Å and 27.4 Å for the **P1**/6-FAM and **P1**/6-TAMRA couples from the spectral overlaps of the donor-acceptor pairs. The 6-TAMRA PL without K^+ might also originate from the intermolecular FRET from 6-FAM to 6-TAMRA in the neighboring molecules (Figure S5, Supporting Information). As shown in **Figure 6**, the two-step FRET-induced PL spectra of aptamer 1 were measured with changing [K^+]. The normalized FRET signal showed a linear dependence on [K^+] in the nanomolar range of [K^+] = 0–50 nM. Substantially enhanced PL signal of 6-TAMRA was observed for all three aptamers due to the light harvesting or optical amplification effect of CPEs. The final 6-TAMRA emission via two-step FRET was enhanced by approximately nine-, seven-, and seven-fold for aptamer 1/**P1**, 2/**P1**, and 3/**P1** sensory systems, respectively, compared to the signal induced by the direct excitation of 6-TAMRA at 566 nm. The excitons generated in the optical units of CPEs migrate through the π-conjugated backbone and can be collected at a specific low energy site via FRET, amplifying the resulting PL signals. FRET-induced 6-TAMRA emission was saturated at [K^+] ≈ 50 nM and the detection limit was determined to be 3.0 nM, 3.6 nM, and 3.9 nM for aptamer 1, 2, and 3 with the addition of **P1** (Figure S6, Supporting Information). The CPE, **P1**, functioned as an optical antenna and improved the LOD dramatically (by 4–6 orders of magnitude), compared to those via 1-step FRET without CPEs. Without CPEs, this sensing scheme works in the millimolar concentration range of K^+ ions and the dynamic detection range was tuned to the nanomolar concentration range by the addition of CPEs ([+]:[-] = 6:1). Interestingly, aptamers 1–3 exhibited similar sensing characteristics by the addition of CPEs with similar FRET signals, LOD and detection range (Figure S6, Supporting Information). A clear signal difference was observed for the three aptameric probes without CPEs due to the different intermolecular separation of 6-FAM and 6-TAMRA in the probe structure. For aptamer 1, the strongest FRET-induced 6-TAMRA emission was measured with the lowest LOD value of 22.5 μM, due to the shorter 6-FAM-6-TAMRA intermolecular separation with compared to aptamer 2 and 3. In contrast, upon the addition of **P1**, the structural flexibility must be limited and two dyes are confined within a limited space (even in the presence of spacers) in the polymeric matrix (Figure S7, Supporting Information). This

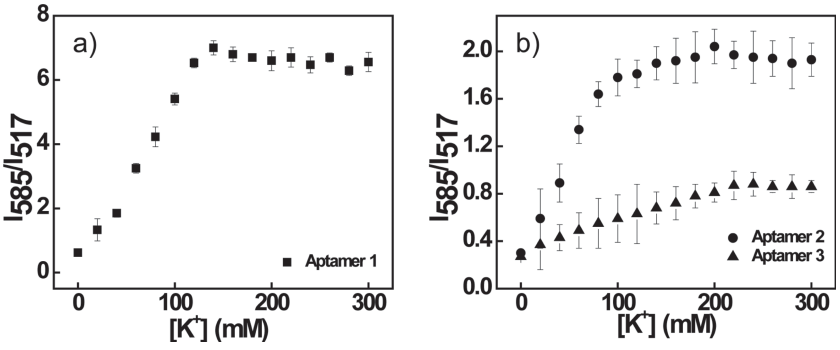

Figure 4. Dynamic detection range of a) aptamer 1 and b) aptamer 2 and 3 based K^+ assays. [Aptamer] = 10 nM in Tris-HCl buffer (20 mM, pH = 7.4).

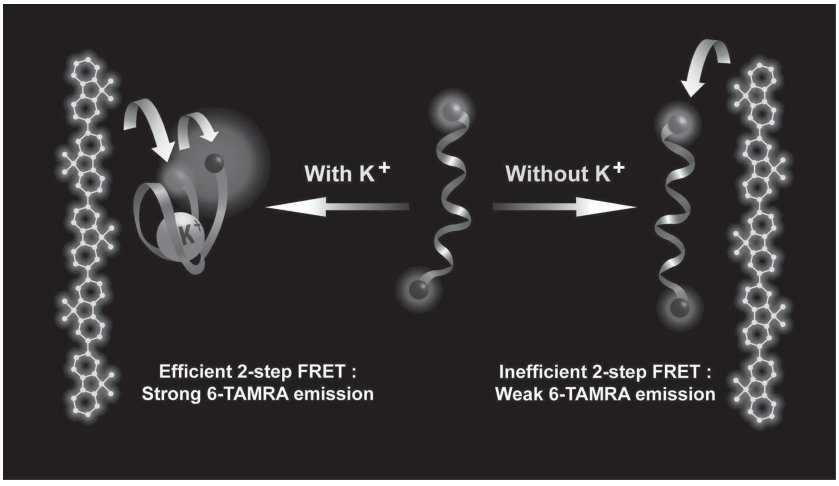

Scheme 3. Two-step FRET based K^+ ion detection.

might induce a decrease in the difference in intermolecular separation (between the two dyes) for the three aptamers and similar sensor characteristics were observed after forming an electrostatic complex with **P1**. In addition, the relative binding strength between the CPE and aptamer, and aptamer and K^+ ions was also tested. First, **P1** was added to the aptamer 1 solution to form an electrostatic complex, aptamer 1/**P1** in 20 mM Tris-HCl buffer, followed by the addition of K^+ ions. After annealing the mixture at 60 °C for 30 min, the PL spectrum was measured by exciting **P1** at 390 nm. Interestingly, the strong 6-TAMRA emission via two-step FRET was obtained similarly, which indicates the formation of the aptamer 1/K^+ quadruplex. This clearly shows that the binding interaction between the aptamer and K^+ is stronger than the interaction between

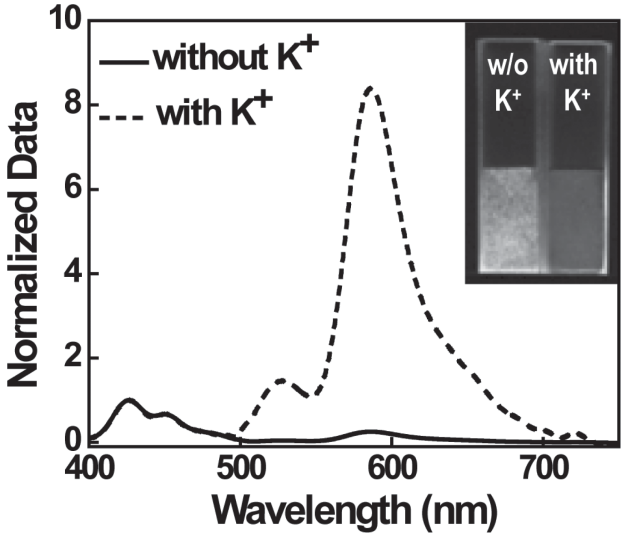

Figure 5. Normalized PL spectra of aptamer 1 upon addition of **P1** with and without K^+ ions. [Aptamer] = 10 nM, [K^+] = 20 mM, [**P1**] = 4.5×10^{-7} M in Tris-HCl buffer (20 mM, pH = 7.4). Excited at 390 nm. Inset shows a photograph of the solution without (left) and with K^+ ions (right) under UV illumination at 365 nm.

the CPE and aptamer (Figure S8, Supporting Information).

The modulation of the detection range and LOD was further extended by controlling the signal amplification effect through adjustments of the **P1** concentration. Without **P1**, K^+ ions (in a millimolar concentration range) were detected successfully with a LOD of 22.5 μM–3.3 mM. In the presence of **P1** (charge ratio of [+]:[-] = 6:1), highly sensitive detection was realized in a range of nanomolar K^+ concentration with a LOD of ≈3 nM. The dynamic detection range was measured at different charge ratios of [+]:[-] = 1:1–6:1. With increasing the charge, the [**P1**] around aptamers increases and more excitons can be transferred to 6-TAMRA with the intensified FRET-induced 6-TAMRA emission. This makes it possible to detect very low concentration of K^+ ions. The modulation of the detection range and LOD is possible by controlling the signal amplification (or antenna) effect of **P1** via simply adjusting the [+]/[-] charge ratio. **Figure 7** shows the dynamic sensor ranges of the aptamer 3/**P1** system with changing the charge ratio. The detection range was successfully tuned from milimolar (at [+]:[-] = 1:1~3:1) to micromolar (at [+]:[-] = 5:1) and nanomolar (at [+]:[-] = 6:1) concentrations with increasing **P1** concentration. Upon the addition of **P1** above [+]:[-] = 6:1, the FRET signal intensity was saturated and the maximum FRET-induced 6-TAMRA emission was measured at [+]:[-] = 6:1.

Figure 8 and Figure S9 (Supporting Information) show the selectivity of this sensory system against a range of other metal ions. The two-step FRET-induced PL signal was measured in the presence of 20 mM NaCl, $CaCl_2$, LiCl, $MgCl_2$, NH_4Cl, $CuCl_2$, AgCl, $ZnCl_2$, and $AlCl_3$ in the same manner used for K^+ detection. Strong FRET-induced 6-TAMRA signal (FRET ratio $I_{585\ nm}/I_{425\ nm} \approx 8$) was measured only in the presence of K^+ ions due to the specific binding affinity to potassium of the G-rich aptamer sequence, showing excellent selectivity against other metal ions. Weak 6-TAMRA emission ($I_{585\ nm}/I_{425\ nm}$ = 0.2–0.3) was observed in the presence of Ca^{2+} and Mg^{2+} ions because Ca^{2+} and Mg^{2+} can also stabilize the G-quadruplex structure. On the other hand, their binding affinity to the aptamers 1–3 was much weaker than that of K^+.[21] A selectivity test for K^+ ions was also performed in the presence of coexisting ions (20 mM). A high FRET ratio of $I_{585\ nm}/I_{425\ nm} \approx 8$ was obtained in the solution containing K^+ and other ions, highlighting the negligible interference from the other ions. The binding affinity between the aptamer and K^+ was not affected by the existence of other ions. These results clearly show that this two-step FRET based sensory system detects K^+ ions selectively against a range of metal ions.

Recently, several research groups reported several approaches to improve the sensor properties for K^+ ions such as sensitivity and selectivity Wang et al. reported the homogeneous potassium detection using fluorescein (Fl) labeled K^+ aptamer and CPE.[20] In the presence of K^+ ion, the random coiled single-stranded aptamer-Fl (weak FRET from CPE to Fl) undergoes the conformational change to G-quadruplex with enhanced Fl

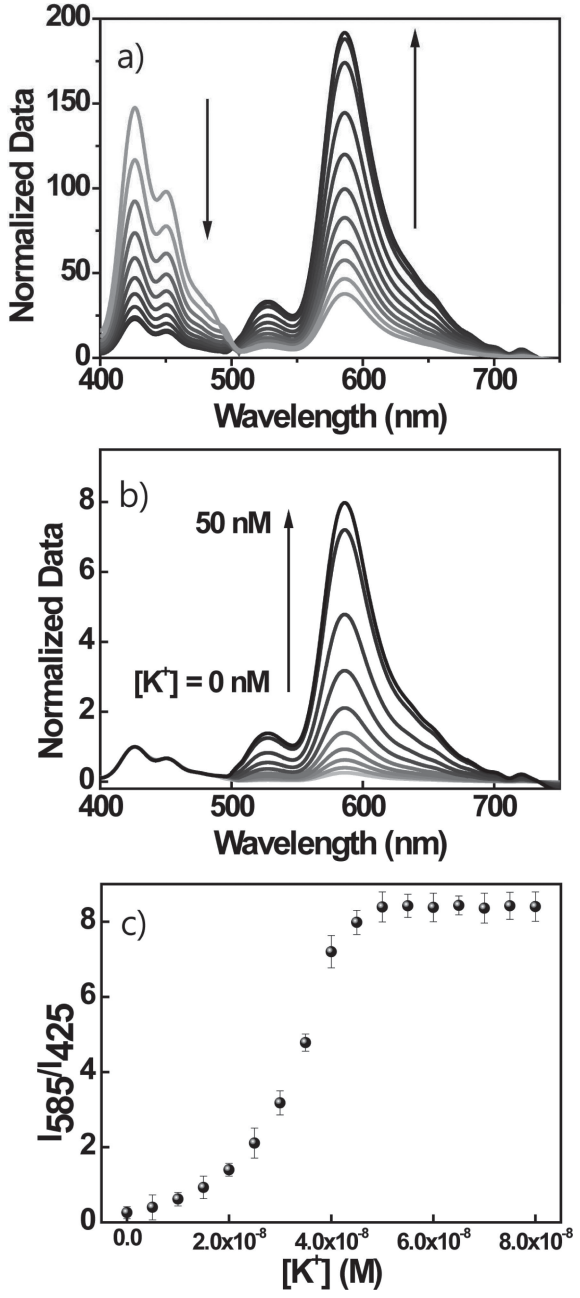

Figure 6. a) Non-normalized and b) normalized two-step FRET induced PL spectra, and (c) FRET ratio for aptamer 1/**P1** based sensory system with increasing [K^+]. [Aptamer 1] = 10 n M, [**P1**] = 4.5 $\times 10^{-7}$ M in Tris-HCl buffer (20 mM, pH = 7.4), excited at 390 nm.

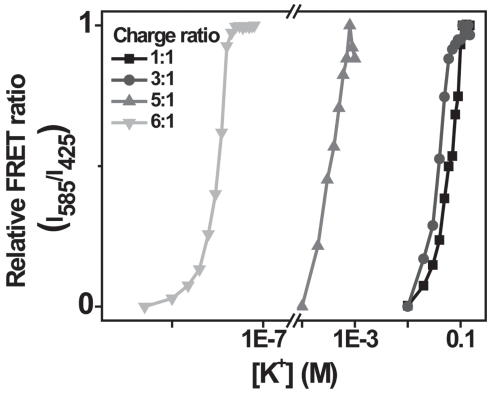

Figure 7. Dynamic detection range of aptamer 3/**P1**-based sensory system with changing the charge ratio ([+] in **P1**:[-] in aptamer). [Aptamer 3] = 10 nM, [**P1**] = 1.5×10^{-7} M ([+]:[-] = 1:1), 4.5×10^{-7} M ([+]:[-] = 3:1), 7.5×10^{-7} M ([+]:[-] = 5:1), 9.0×10^{-7} M ([+]:[-] = 6:1) in Tris-HCl buffer (20 mM, pH = 7.4).

emission. However, a weak FRET signal was observed even in the absence of K^+ due to the electrostatic interaction between DNA and the cationic CPE, which makes relatively low on/off ratio. We also suggested a molecular beacon aptamer (MBA)-based potassium detection strategy.[6] The CPE-triggered conformational change of MBA (labeled with a fluorophore and quencher at both termini) to an open chain is hindered due to the G-quadruplex formation with K^+ ions, resulting in PL quenching. Although this potassium assay is highly sensitive (LOD ≈ 1.5 nM) and selective, the PL signal turn off with K^+, which has some difficulties for biological imaging applications. In this two-step based scheme, we successfully realized highly sensitive (LOD ≈ 3 nM) and selective sensing for K^+ ions using a turn-on scheme. In addition, the characteristic to tune detection ranges by modulating the antenna effect of CPE makes our system useful for practical applications. More importantly, this sensing scheme might be able to detect a wide range of target species that can form a G-quadruplex with an aptamer, by simply modifying the specific base sequence of the aptamer.

Finally we also tested the K^+ detection in a Bovine serum albumin (BSA) solution. The BSA solution (0.5–5.0 wt%) was prepared by following the procedures reported previously.[22] We measured the clear turn on and off signals in the presence and absence of K^+ ions via two-step FRET (**Figure 9**). However, the FRET-induced 6-TAMRA emission was somewhat decreased with compared to those in Tris-HCl buffer. This is probably due to the electrostatic interaction between **P1** and BSA. The isoelectric point of BSA is 4.8 and it must be negatively charged in Tris-HCl buffer (pH 7.4). The complexation of **P1**/BSA may influence the formation of the electrostatic complex, aptamer/**P1** and the resulting antenna effect of **P1** in the two-step sensor scheme.

3. Conclusions

A new sensing strategy for K^+ ions was developed by combining the high binding specificity of a biosystem (aptamer) and a synthetic polymer with tunable optical amplifications. Highly sensitive and selective K^+ detection was demonstrated via single- and two-step FRET processes with a tunable sensing range and LOD. Three K^+-specific aptamers were designed as a probe, which was labeled with 6-FAM and 6-TAMRA at both ends with different spacer groups between them. Suitable distance control allows efficient FRET between the dyes, showing the successful tuning of the sensor characteristics. FRET-induced 6-TAMRA emission was proportional to [K^+] in a range of 22.5 μM–100 mM in the presence of excess Na^+ ions (100 mM). Upon the addition

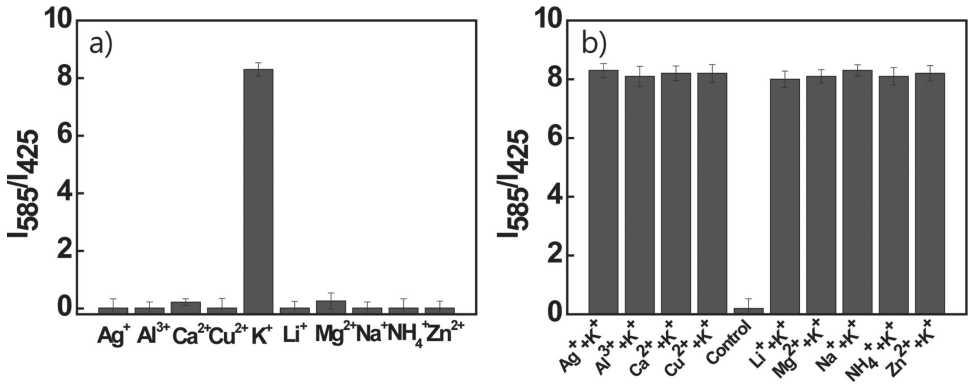

Figure 8. a) Selectivity of aptamer 1/**P1** based sensory system against a range of other metal ions. b) Selectivity data for potassium ion in the presence of coexisting metal ions. [Aptamer 1] = 10 nM, [Metal ions] = 20 mM, [**P1**] = 4.5×10^{-7} M in Tris-HCl buffer (20 mM, pH = 7.4). (Control: without K^+ ions).

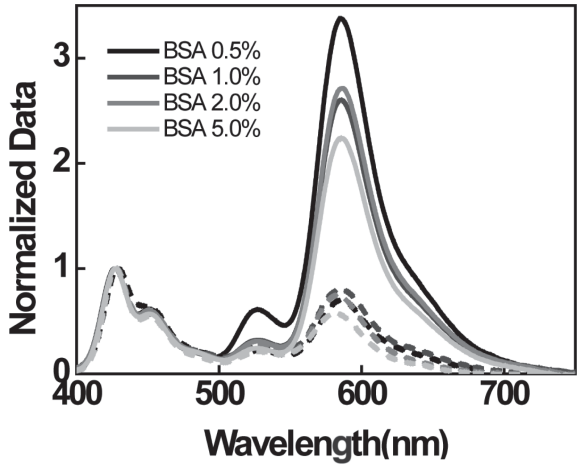

Figure 9. Normalized PL spectra in the presence (solid) and absence (dashed) of K^+ ions in a BSA solution via the two-step FRET process. [Aptamer 1] = 10 nM, [K^+] = 50 nM, [**P1**] = 4.5×10^{-7} M in Tris-HCl buffer (20 mM, pH = 7.4).

of CPE, a two-step FRET process was enabled from CPE to 6-TAMRA via 6-FAM, showing an intensified 6-TAMRA signal with K^+ ions. The dynamic detection range was extended from the ~millimolar to ~micromolar range and ~nanomolar concentration of K^+ by modulating the signal amplification effect of CPE. The LOD of ≈3.0 nM was measured with high selectivity against other metal ions. It is noteworthy to mention that this sensing scheme can be extended to the detection of other target materials by simply modifying the recognition aptamer sequence.

4. Experimental Section

General: All chemicals were purchased from Aldrich Chemical Co. and used as received unless otherwise mentioned. Three kinds of high pressure liquid chromatography (HPLC)-purified molecular aptamers labeled with 6-FAM and 6-TAMRA with 15 bases (aptamer 1: 5′-6-FAM-GGTT GGTG TGGT TGG-6-TAMRA-3′), 20 bases (aptamer 2: 5′-6-FAM-TTTT AGGT TGGT GTGG TTGG-6-TAMRA-3′) and 30 bases (aptamer 3: 5′-6-FAM-TTTT ATTT TAGG TTGG TGTG GTTG GTTT TA-6-TAMRA-3′) for sensing K^+ ions were obtained from Sigma-Genosys. ^{1}H- and ^{13}C-NMR spectra were recorded on a JEOL (JNM-AL300) FT NMR system operating at 300 MHz (or 400 MHz) and 75 MHz (or 100 MHz), respectively. The number- and weight-average molecular weights of the polymer were determined by gel permeation chromatography (GPC) with chloroform as an eluent using Agilent GPC 1200 series, relative to polystyrene as a standard. UV-vis spectra were measured on a Jasco V-630 UV-vis spectrometer. The photoluminescence (PL) spectra were obtained on a Jasco (FP-6500) spectrofluorometer with a xenon lamp excitation source, using 90 ° angle detection for solution samples. The PL quantum yield of the polymer was measured relative to a freshly prepared fluorescein solution in water at pH = 11.

Synthesis of 2,7-Bis(4,4,5,5-tetramethyl-1,3,2-dioxaborolan-2-yl)-9,9-bis(6′-bromohexyl)fluorene (1): Compound 1 was synthesized by following the procedures reported previously.[23] Yield: 0.95 g (42%). ^{1}H NMR (300 MHz, $CDCl_3$, δ): 7.82 (d, 2H, J = 7.5Hz), 7.73 (m, 4H), 3.34 (t, 4H, J = 6.9Hz), 2.02 (m, 4H), 1.62 (m, 4H), 1.39 (s, 24 H), 1.17 (m, 4H), 1.04 (m, 4H), 0.55 (m, 4H). ^{13}C NMR (75 MHz, $CDCl_3$, δ): 150.27, 144.09, 133.99, 128.93, 119.67, 83.97, 55.24, 40.12, 34.19, 32.84, 29.15, 27.93, 23.55. Anal.calcd for $C_{36}H_{52}B_2Br_2O_4$: C, 59.21; H, 7.18; B, 2.96; Br, 21.88. Found: C, 59.31; H, 7.21.

Synthesis of 2,7-Dibromo-9,9-bis(3,4-dihydroxyphenyl)fluorene (2): To a mixture of pyrocatechol (1.5 g, 13.6 mmol), 2,7-dibromofluorenone (2.0 g, 5.92 mmol) and 3-mercaptopropionic acid (1 mL) was added concentrated sulfuric acid (0.5 mL) slowly at 80 °C. The reaction mixture was stirred for 2 h at 80 °C and quenched by adding toluene. The precipitate was washed with hot water several times and filtered. After drying, the products were used in the next experiment without further purification. Yield: 86% (2.76 g). ^{1}H-NMR (300 MHz, $CDCl_3$, δ): 8.90 (d, 4H), 7.87 (d, 2H), 7.56 (d, 2H), 7.45 (s, 2H), 6.64 (d, 2H), 6.52 (s, 2H), 6.35 (d, 2H). ^{13}C-NMR (75 MHz, $CDCl_3$, δ): 153.87, 144.94, 137.58, 135.07, 130.56, 128.92, 128.22, 125.33, 122.71, 120.98, 118.54, 115.25, 64.15.

Synthesis of 2,7-dibromo-9,9-bis(3,4-bis(2-(2-methoxyethoxy)ethoxy) phenyl)fluorene (3): To a mixture of compound 2 (1.0 g, 1.9 mmol), K_2CO_3 (3.0 g, 21.7 mmol) and KI (0.15 g, 0.9 mmol) in acetone (20 mL) was added 1-bromo-2-(2-methoxyethoxy)ethane (2.0 g, 10.9 mmol). The reaction mixture was refluxed for 2 days and cooled down to room temperature. The precipitate was removed by filtration and the filtrate was concentrated under reduced pressure. The residue was extracted with methylene chloride, washed with water several times and dried over magnesium sulfate. After drying, the product was purified by column chromatography on silica gel with hexane/ethyl acetate (1/1, v/v) to give a product. Yield: 63% (1.1 g). ^{1}H-NMR (400 MHz, $CDCl_3$, δ): 7.45 (d, 2H, J = 8.0 Hz), 7.36 (m, 4H), 6.67 (m, 4H), 6.53 (d, 2H, J = 8.4 Hz), 4.04 (t, 4H, J = 5.2 Hz), 3.94 (t, 4H, J = 5.2 Hz), 3.74 (t, 4H, J = 5.2 Hz), 3.70 (t, 4H, J = 5.2 Hz), 3.54 (m, 8H), 3.44 (m, 8H),

3.27 (s, 12H). ^{13}C-NMR (100 MHz, $CDCl_3$, δ): 153.01, 148.30, 148.11, 137.60, 137.10, 130.67, 128.91, 121.48, 121.44, 120.76, 115.17, 113.81, 71.73, 71.67, 70.46, 69.46, 69.39, 68.73, 68.48, 64.52, 58.76. Anal.calcd for $C_{45}H_{56}Br_2O_{12}$: C, 56.97; H, 5.95; Br, 16.84. Found: C, 57.11; H, 5.99.

Polymerization and Quaternization: To a mixture of monomer 1 (0.164 g, 0.220 mmol), 3 (0.209 g, 0.220 mmol) and 15 mg of $(PPh_3)_4Pd(0)$ were added 2 M aqueous potassium carbonate (4 mL, N_2purged) and the phase transfer catalyst, Aliquat 336 in toluene (8 mL, N_2purged). The reaction mixture was heated at 85 °C for 24 h, excess bromobenzene in 1 mL toluene (N_2purged) was added as an end capper, and further reacted for another 12 h. The reaction mixture was cooled down to room temperature and precipitated into vigorously stirred methanol (200 mL). The polymer fibers were collected by filtration and washed for 2 days in a Soxhlet apparatus with acetone to remove oligomers and catalyst residues. The neutral precursor polymer was obtained after drying in vacuo. Yield: 66% (186 mg). M_n= 25 000 g mol^{-1} (M_w/M_n= 1.26). The quaternization of the neutral precursor was followed with trimethylamine.[24] Condensed trimethylamine (3–5 mL) was added dropwise to a solution of the neutral precursor (100 mg) in 10 mL THF at –78 °C. The mixture was allowed to warm up to room temperature overnight. The precipitate was re-dissolved by addition of methanol and 2 mL trimethylamine was added at –78 °C. The resulting mixture was stirred for additional 24 h at room temperature. After removal of the solvent under reduced pressure, acetone was added to precipitate the charged polymer (P1). The precipitated P1 was then collected and dried under vacuum. Yield: 85% (93 mg). ^{1}H NMR (300 MHz, DMSO-d_6, δ): 8.36 (s, 2H), 7.80–7.62 (br, 6H), 7.22 (br, 6H), 6.92 (br, 4H), 4.03 (br, 6H), 3.69 (br, 8H), 3.41 (br, 10H), 3.02 (s, 18H), 2.11 (br, 10H), 1.66 (br, 4H), 1.41 (br, 18H), 1.04 (br, 12H).

Potassium Ion Assay Protocol: All PL experiments were performed in 20 mM Tris-HCl buffer (pH = 7.4) containing 100 mM NaCl as a salt. Stock solutions (10^{-6} M) of 3 kinds of potassium aptamers were prepared in deionized water. 20 µL of the aptamer stock solution was diluted to 2 mL buffer, and the resulting solution was incubated at 60 °C for 30 min with and without K^+ ions. The annealed solution was cooled down to room temperature for 1 h and the PL spectra were measured by exciting 6-FAM at 490 nm. Then, P1 was added to the above solution and PL spectra were measured again by exciting the polymer at 390 nm. The same protocol was repeated in the presence of NaCl, $CaCl_2$, LiCl, $MgCl_2$, NH_4Cl, $CuCl_2$, AgCl, $ZnCl_2$, and $AlCl_3$ (20 mM, respectively) instead of KCl for the selectivity evaluation.

Supporting Information

Supporting Information is available from the Wiley Online Library or from the author.

Acknowledgments

B.L.N. and J.-E.J. contributed equally to this work. This work was supported by Basic Science Research Program through the National Research Foundation (NRF) of Korea (2012R1A2A2A06045327, 2012M3A6A7055540, 2012K1A2B1A03000406, BRL 2011–0001198).

Received: May 3, 2013
Revised: July 4, 2013
Published online: November 4, 2013

[1] a) D. T. McQuade, A. E. Pullen, T. M. Swager, *Chem. Rev.* **2000**, *100*, 2537–2574; b) S. W. Thomas III, G. D. Joly, T. M. Swager, *Chem. Rev.* **2007**, *107*, 1339–1386; c) H. Jiang, P. Taranekar, J. R. Reynolds, K. S. Schanze, *Angew. Chem. Int. Ed.* **2009**, *48*, 4300–4316; d) A. Duarte, K.-Y. Pu, B. Liu, G. C. Bazan, *Chem. Mater.* **2011**, *23*, 501–515.

[2] a) Q. Zhou, T. M. Swager, *J. Am. Chem. Soc.* **1995**, *117*, 7017–7018; b) T. M. Swager, *Acc. Chem. Res.* **1998**, *31*, 201–207.

[3] a) J. Liang, K. Li, B. Liu, *Chem. Sci.* **2013**, *4*, 1377–1394; b) C. A. Traina, R. C. Bakus II, G. C. Bazan, *J. Am. Chem. Soc.* **2011**, *133*, 12600–12607; c) K. Lee, L. K. Povlich, J. Kim, *Adv. Funct. Mater.* **2007**, *17*, 2580–2587; d) H. A. Ho, M. Leclerc, *J. Am. Chem. Soc.* **2004**, *126*, 1384–1387; e) H. Fan, T. Zhang, S. Lv, Q. Jin, *J. Mater. Chem.* **2010**, *20*, 10901–10907; f) X. Feng, X. Duan, L. Liu, F. Feng, S. Wang, Y. Li, D. Zhu, *Angew. Chem. Int. Ed.* **2009**, *48*, 5316–5321.

[4] a) L. C. Bock, L. C. Griffin, J. A. Latham, E. H. Vermaas, J. J. Toole, *Nature* **199 2**, *355*, 364–366; b) T. Hermann, D. J. Patel, *Science* **2000**, *287*, 820–825; c) S. D. Jayasena, *Clin. Chem.* **1999**, *45*, 1628–1650.

[5] a) J. T. Davis, *Angew. Chem. Int. Ed.* **2004**, *43*, 668–698; b) Y. Xu, H. Sugiyama, *Nucleic Acids Res.* **2006**, *34*, 949–954; c) V. T. Mukundan, A. T. Phan, *J. Am. Chem. Soc.* **2013**, *135*, 5017–5028.

[6] a) T. Shigeori, J. Bernard, *Anal. Sci.* **2011**, *27*, 1167–1172; b) B. Kim, I. H. Jung, M. Kang, H.-K. Shim, H. Y. Woo, *J. Am. Chem. Soc.* **2012**, *134*, 3133–3138.

[7] a) Y. Wang, B. Liu, *Langmuir* **2009**, *25*, 12787–12793; b) N. Li, C. M. Ho, *J. Am. Chem. Soc.* **2008**, *130*, 2380–2381; c) S. Yan, R. Huang, Y. Zhou, M. Zhang, M. Deng, X. Wang, X. Weng, X. Zhou, *Chem. Commun.* **2011**, *47*, 1273–1275; d) R. Nutiu, Y. Li, *Angew. Chem. Int. Ed.* **2005**, *44*, 1061–1065.

[8] a) M. Cermirana, T. M. Desai, M. Sadqi, V. Munoz, *J. Am. Chem. Soc.* **2012**, *134*, 8010–8013; b) A. Vallée-Beslisle, F. Ricci, K. W. Plaxco, *Proc. Natl. Acad. Sci. U. S. A.* **2009**, *106*, 13802–13807.

[9] a) A. Vallée-Beslisle, F. Ricci, K. W. Plaxco, *J. Am. Chem. Soc.* **2012**, *134*, 2876–2879; b) A. Porchetta, A. Vallée-Beslisle, K. W. Plaxco, F. Ricci, *J. Am. Chem. Soc.* **2012**, *134*, 20601–20604; c) F. Ricci, A. Vallée-Beslisle, A. Porchetta, K. W. Plaxco, *J. Am. Chem. Soc.* **2012**, *134*, 15177–15180.

[10] a) L. Li, X. Shen, Q.-H. Xu, S. Q. Yao, *Angew. Chem. Int. Ed.* **2013**, *125*, 442–446; b) B. Sacca, R. Meyer, U. Feldkamp, H. Schroeder, C. M. Niemeyer, *Angew. Chem. Int. Ed.* **2008**, *47*, 2135–2137; c) B. S. Gaylord, M. R. Massie, S. C. Feinstein, G. C. Bazan, *Proc. Natl. Acad. Sci. U. S. A.* **2005**, *102*, 34–39.

[11] a) J. Liu, Y. Lu, *J. Am. Chem. Soc.* **2002**, *124*, 15208–15216; b) H. M. Watrob, C. P. Pan, M. D. Barkley, *J. Am. Chem. Soc.* **2003**, *125*, 7336–7343; c) S. H. Kim, J. R. Gunther, J. A. Katzenellenbogen, *J. Am. Chem. Soc.* **2010**, *132*, 4685–4692; d) I. Horsey, W. S. Furey, J. G. Harrison, M. A. Osborne, S. Balasubramanian, *Chem. Commun.* **2000**, 1043–1044; e) A. Aneja, N. Marthur, P. K. Bhatnagar, P. C. Mathur, *J. Biol. Phys.* **2008**, *34*, 487–493.

[12] S. P. Yu, L. M. Canzoniero, D. W. Choi, *Curr. Opin. Cell Biol.* **2001**, *13*, 405–411.

[13] a) W. Walz, *Neurochem. Int.* **2000**, *36*, 291–300; b) S. J. Lippard, J. M. Berg, in *Principles of Bioinorganic Chemistry*, University Science Books: Mill Valley, CA, USA, **1994**, Ch. *1*; c) H.-C. Kuo, C.-F. Cheng, R. B. Clark, J. J.-C. Lin, J. L.-C. Lin, M. Hoshijima, V. T. B. Nguyen-Tran, Y. Gu, Y. Ikeda, P.-H. Chu, J. Ross Jr., W. R. Giles, K. R. Chien, *Cell* **2001**, *107*, 801–813.

[14] a) J. Kim, D. T. McQuade, D. Tyler, S. K. McHugh, T. M. Swager, *Angew. Chem. Int. Ed.* **2000**, *39*, 3868–3872; b) V. S. Le, B. Kim, W. Lee, J.-E. Jeong, R. Yang, H. Y. Woo, *Macromol. Rapid Commun.* **2013**, *34*, 772–778.

[15] K. Y. Pu, B. Liu, *Macromolecules* **2008**, *41*, 6636–6640.

[16] a) J. W. Hong, H. Benmansour, G. C. Bazan, *Chem. Eur. J.* **2003**, *9*, 3186–3192; b) R. Yang, A. Garcia, D. Korystov, A. Mikhailovsky, G. C. Bazan, T. Q. Nguyen, *J. Am. Chem. Soc.* **2006**, *128*, 16532–16539.

[17] a) M. Stork, B. S. Gaylord, A. J. Heeger, G. C. Bazan, *Adv. Mater.* **2002**, *14*, 361–366; b) F. Xia, X. Zuo, R. Yang, Y. Xiao, D. Kang, A. Vallée-Beslisle, X. Gong, A. J. Heeger, K. W. Plaxco, *J. Am. Chem. Soc.* **2010**, *132*, 1252–1254.

[18] a) M. Kang, O. K. Nag, S. Hwang, I. Kim, H. Yang, K. Kyhm, H. Y. Woo, *Phys. Chem. Chem. Phys.* **2010**, *12*, 15482–15489; b) X. Feng, F. Lv, L. Liu, Q. Yang, S. Wang, G. C. Bazan, *Adv. Mater.* **2012**, *24*, 5428–5432.

[19] H. M. Kim, H.-J. Choo, S.-Y. Jung, Y.-G. Ko, W.-H. Park, S.-J. Jeon, C. H. Kim, T. Joo, B. R. Cho, *ChemBioChem* **2007**, *8*, 553–559.

[20] F. He, Y. Tang, S. Wang, Y. Li, D. Zhu, *J. Am. Chem. Soc.* **2005**, *127*, 12343–12346.

[21] C. C. Hardin, T. Watson, M. Corregan, C. Bailey, *Biochemistry* **1992**, *31*, 833–841.

[22] a) Y. Zhong, F. Peng, F. Bao, S. Wang, X. Ji, L. Yang, Y. Su, S.-T. Lee, Y. He, *J. Am. Chem. Soc.* **2013**, *135*, 8350–8356; b) Y. Wang, R. Zhan, T. Li, K.-Y. Pu, Y. Wang, Y. C. Tan, B. Liu, *Langmuir* **2012**, *28*, 889–895; c) K.-Y. Pu, J. Shi, L. Cai, K. Li, B. Liu, *Biomacromolecules* **2011**, *12*, 2966–2974; d) L. J. Nielsen, L. F. Olsen, V. C. Ozalp, *ACS Nano* **2010**, *4*, 4361–4370.

[23] a) B. Liu, G. C. Bazan, *Chem. Asian J.* **2007**, *2*, 499–504; b) B. Liu, G. C. Bazan, *J. Am. Chem. Soc.* **2006**, *128*, 1188–1196.

[24] H. Y. Woo, D. Vak, D. Korystov, A. Mikhailovsky, G. C. Bazan, D. Y. Kim, *Adv. Funct. Mater.* **2007**, *17*, 290–295.